Interrogation of Fluctuating Tumour Microvasculature Using Combined Carbogen-USPIO (CUSPIO) Imaging

J. S. Burrell[1], J. C. Waterton[2], A. Ryan[2], S. P. Robinson[1], and S. Walker-Samuel[1]

[1]The Institute of Cancer Research, London, Sutton, United Kingdom, [2]AstraZeneca, Cheshire, United Kingdom

Introduction: MRI is sensitive to changes in tissue magnetic susceptibility, which can be utilised in the investigation of tumour microvasculature [1]. R_2* decreases with hyperoxia due to the difference in susceptibility between deoxy- and oxyhaemoglobin (deoxyhaemoglobin is paramagnetic, oxyhaemoglobin is diamagnetic). Conversely, ultrasmall paramagnetic iron oxide (USPIO) particle contrast agents induce an increase in R_2* and, for a known blood plasma concentration, can be used to estimate tumour blood volume. Due to the difference in size of erythrocytes and USPIO particles, (~6µm and 30nm respectively [2]), the volume of distribution influenced by hyperoxia and USPIO is likely to differ, with small vessels offering preferential access to USPIO. Carbogen (5% CO_2, 95% O_2) additionally may induce vascular steal (potentially causing an *increase* in R_2* during carbogen breathing [3]) and transient hypoxia [4] which can be probed using carbogen and USPIO in combination. In this study, tumours derived from two human colorectal cell lines were investigated by combined carbogen-USPIO (CUSPIO) imaging. Differences in the magnitude and spatial distribution of R_2* changes induced by carbogen and USPIO were investigated and temporal fluctuations in perfusion evaluated.

Methods: *Data Acquisition:* In compliance with licenses issued under the UK Animals (Scientific Procedures) Act, six female NCr nude mice were injected subcutaneously on the right flank with 5×10^6 HCT116 or SW1222 cells. The tumours were imaged one week later at a diameter of approximately 1cm. All images were acquired on a 7T horizontal bore Bruker system using a 3cm birdcage coil. The mice were restrained using dental paste in order to limit motion artefacts [5]. TurboRARE images were acquired for tumour delineation, followed by two baseline multi gradient echo MGE acquisitions (3 contiguous 1mm slices, TR=200msec, TE=6–28ms, 4ms echo spacing, 8 averages) acquired during air breathing. The air supply was then switched to carbogen delivered via a nosepiece. Following a two minute transition time, a further identical MGE image set was acquired. The gas supply was then reverted to air and, after a 10 minute transition time, a second baseline MGE image set was acquired. A final MGE image set was acquired one minute after the injection of 150µmol/kg USPIO contrast agent ferumoxtran-10 (Sinerem®, Guerbet) via a cannulated tail vein. *Data Analysis:* MGE data were fitted using a Bayesian maximum *a posteriori* approach [6]. This modelled the MGE signal magnitude as a single exponential decay and took into account its Rician noise distribution. Furthermore, it enabled estimates of ΔR_2* uncertainty ($\sigma_{\Delta R2*}$) to be defined and the probability that a given ΔR_2* estimate was significantly greater than or less than zero. Thus, the number of pixels within the tumour ROI with $\sigma_{\Delta R2*}$<0.05/ms and with a significant change in R_2* due to carbogen (ΔR_2*_{carbo}) and/or USPIO (ΔR_2*_{USPIO}) ($p<0.05$) were calculated, for tumours from each cell line. RGB maps were generated with a red channel designated to pixels with a positive ΔR_2*_{carbo}, the blue channel to pixels with negative ΔR_2*_{carbo} and the green channel to positive ΔR_2*_{USPIO}. Regions with both negative ΔR_2*_{carbo} and positive ΔR_2*_{USPIO} therefore appeared cyan (blue + green) and regions with both positive ΔR_2*_{carbo} and positive ΔR_2*_{USPIO} appeared yellow (red + green). Fractional blood volume was quantified from ΔR_2*_{USPIO} data using the method of Gambarota *et al* [7].

Results and Discussion: Mean fractional blood volume for SW1222 tumours was 8.9%, compared with 3.9% for HCT116 tumours. This result agrees with previous reports of raised vascular volumes in SW1222 tumours [8]. **Table 1** shows the percentage of tumour pixels from each cell line that exhibited various categories of change in R_2* (for $p<0.05$). The colour associated with each category of change corresponds to pixels in the colour maps shown in **figure 1**. The percentage of pixels which displayed a positive ΔR_2*_{USPIO} (green) was significantly higher in SW1222 than in HCT116, which mirrors the measurement of their raised blood volume. A greater percentage of pixels from SW1222 tumours displayed a positive ΔR_2*_{USPIO} and positive ΔR_2*_{carbo} (cyan) compared with HCT116 tumours. Such regions exhibited increased oxygenation during carbogen administration and were also perfused during the USPIO phase, which is the expected response. However, of the two tumour types, approximately equal numbers of pixels showed a positive ΔR_2*_{USPIO} and ΔR_2*_{carbo} (yellow).These regions become less oxygenated during the carbogen breathing phase (potentially due to vascular steal or transient hypoxia) but were reperfused during the USPIO phase. Similarly regions with insignificant ΔR_2*_{USPIO} and either positive or negative ΔR_2*_{carbo} (red and blue, respectively) varied in oxygenation during carbogen but subsequently precluded access to USPIO. We interpret this as reflecting vascular shutdown following or during the carbogen-breathing phase.

Inspection of **figure 1** reveals that HCT116 tumours displayed a greater heterogeneity of R_2* response, which is reflected in the values shown in **table 1**. Regions that were significantly perturbed by carbogen in SW1222 tumours were typically also perfused by USPIO, and a greater proportion of pixels displayed the expected negative ΔR_2*_{carbo}. Conversely, HCT116 tumours showed large regions that were perturbed by carbogen, but not accessible to USPIO, and a greater proportion of pixels that exhibited a positive ΔR_2*_{carbo}. This suggests that HCT116 produces a haemodynamic phenotype more susceptible to transient vascular shutdown and intra-tumour or systemic vascular steal effects. These imaging data are consistent with previous histological data using the double fluorescent probe technique employed by Trotter *et al* in their study of transient perfusion in murine tumours [9].

Table 1. Categorisation of ΔR_2* for tumour ROI's (n/s = not significant, p>0.05)

	Colour	Percentage of tumour pixels (SW1222)	Percentage of tumour pixels (HCT116)
$\Delta R_2*_{USPIO} > 0$	GREEN	**86.0**	**49.5**
$\Delta R_2*_{USPIO} >0$; $\Delta R_2*_{carbo} <0$	CYAN	**31.9**	**16.1**
$\Delta R_2*_{USPIO} >0$; $\Delta R_2*_{carbo} >0$	YELLOW	**23.6**	**18.5**
ΔR_2*_{USPIO} n/s ; $\Delta R_2*_{carbo} >0$	RED	**4.9**	**21.0**
ΔR_2*_{USPIO} n/s ; $\Delta R_2*_{carbo} <0$	BLUE	**4.7**	**13.0**

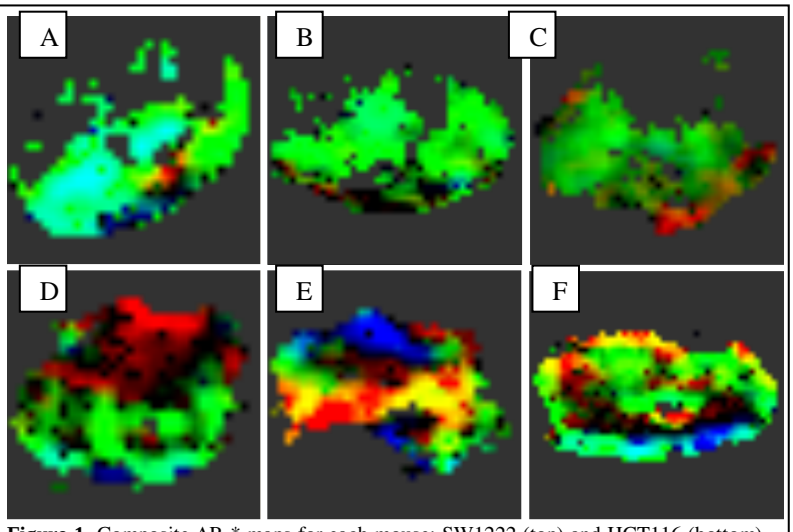

Figure 1. Composite ΔR_2* maps for each mouse; SW1222 (top) and HCT116 (bottom). Green = positive ΔR_2*_{USPIO}, blue = negative ΔR_2*_{carbo}, red = positive ΔR_2*_{carbo}, Yellow = red + green, cyan = blue + green. Black regions represent no change in R_2*

Conclusion: CUSPIO imaging revealed differences in the vascular stability of SW1222 and HCT116 tumours. This has implications for their use in drug efficacy studies as large regions of HCT116 tumours can become isolated from a vascular supply. This study suggests that CUSPIO imaging can detect transient vascular shutdown *in vivo*. Further work is required to evaluate the duration of such fluctuations and to investigate the influence of vascular patency on transient tumour perfusion.

Acknowledgements: This work was supported by BBSRC, AstraZeneca, The Royal Society, Cancer Research UK grant number C1060/A5117 and also NHS funding to the NIHR Biomedical Research Centre.

References: 1) Robinson et al, JMRI, 2003, **17**(4) 445. 2) Jung et al, MRI, 1995, **13**(5) 661 3) Karczmar et al., NMR Biomed, 1994, **7**(1-2) 3 4) Lanzen et al, Cancer Res, 2006, **66**(4) 2219 5) Landuyt et al, JMRI, 2002, **16**(2) 224 6) Walker-Samuel et al, in *Proc ISMRM Cancer Workshop*. 2008. Nice. 7) Gambarota et al, MRI, 2006, **24**(3) 279 8) El Emir et al, Cancer Res 2007, **67**(24) 11896. 9) Trotter et al, IJROBP 1989, **16**(4) 931.